DESY-05-083
hep-ph/0506047

Off-Shell Scattering Amplitudes for WW Scattering and the Role of the Photon Pole

J. Bartels and F. Schwennsen

II. Institut für Theoretische Physik, Universität Hamburg
Luruper Chaussee 149, D-22761 Hamburg, Germany

Abstract

We derive analytic expressions for high energy $2 \to 2$ off-shell scattering amplitudes of weak vector bosons. They are obtained from six fermion final states in processes of the type $e^+e^- \to \bar{\nu}_e + (WW) + \nu_e \to \bar{\nu}_e + (l\nu)(l\nu) + \nu_e$. As an application we reconsider the unitarity bounds on the Higgs mass. Particular attention is given to the role of the photon exchange which has not been considered in earlier investigations; we find that the photon weakens the bound of the Higgs mass.

1 Introduction

The elastic scattering of weak vector bosons plays a central role in our understanding of the electroweak sector of the standard model. It is known that, without any Higgs, these scattering processes have a bad high energy behavior, i.e. they start to violate, at energies of about $\sim$ 1TeV, bounds derived from unitarity. The Higgs mechanism cures this defect; but if the Higgs mass is larger than about $\sim$ 1TeV [1], the weak sector becomes strongly interacting, and the use of low order perturbation theory becomes insufficient. So there is little doubt that the high energy behavior of heavy vector boson scattering carries much information on the electroweak symmetry breaking.

Although the field has already a rather long history [2, 3, 4, 5, 6, 7, 8], there still remain aspects which deserve further studies. One is the stability of the heavy vector bosons in the electroweak sector. Most of the existing studies consider the scattering of on-shell vector mesons, i.e. the heavy gauge boson is treated as a stable particle. A more realistic investigation has to include both the production and the decay of the bosons which necessarily leads to off-shell bosons, both in the initial and in the final state. Secondly, a full analysis of boson scattering in the electroweak sector includes the photon:

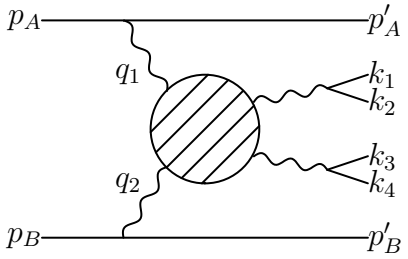

Figure 1: $e^+e^- \to 6f$.

because of the photon pole in the t-channel, on-shell vector boson scattering, strictly speaking, is not defined in the forward direction. In this paper, we attempt to address some of these issues in the framework of more 'realistic' off-shell scattering processes.

One of the possibilities of embedding vector scattering, e.g. the elastic scattering of two W bosons, into a 'realistic' process is the six fermion process $e^+e^- \to 6f$: (Fig.1). In order to isolate 'incoming' W bosons for the WW scattering subprocess, one has to consider the process $e^+e^- \to 6f$ in the restricted kinematic region where the produced WW pair lies in the central region, i.e. in rapidity it is well-separated from the fragments of the incoming leptons, the ν_e and the $\bar{\nu}_e$. In this region the t-channel W's serve as incoming bosons: they are radiated off the incoming electron and positron, and their momenta are spacelike and off-shell. Also the 'outgoing' W bosons are off shell, but, in contrast to the 'incoming' W bosons, they have timelike momenta. In order to simulate WW scattering at high energies, we need the subenergy of the WW subprocess to be as large as possible. A computer-based analysis of this class of six-fermion processes has been given in [9]. In our paper we derive analytic expressions for the vector scattering subprocesses which can be used for further theoretical investigations. As an example, we will study the influence of the Higgs particle on the high energy behavior of WW scattering; an aspect of particular interest is the role of the photon pole in the unitarity bound.

In section 2 we derive expressions for the process $e^+e^- \to 6f$ which are valid in the kinematic region described above. In section 3 we discuss a unitarity condition for the WW scattering subprocess, and we discuss the role of the photon pole. We also comment on the role of the instability of the W boson in the unitarity equation.

2 The processes $e^+e^- \to 6f$

We begin with elastic WW - scattering which appears as a subprocess of the reaction $e^+e^- \to \nu_e\, 4f\, \bar{\nu}_e$. Our notations are indicated in Fig.1, and a few diagrams are illustrated in Fig.2. In particular, $s = (p_A + p_B)^2$ denotes the squared energy of incoming electrons, and $\hat{s} = (q_1 + q_2)^2$ the mass squared of the produced WW system. In order to obtain a meaningfull off-shell extension of high energy WW scattering, we consider the so-called multi-Regge limit: the squared masses of the "incoming" W-momenta, $t_1 = q_1^2$ and $t_2 = q_2^2$, and of the "outgoing" momenta, $M_1^2 = (k_1 + k_2)^2 \equiv k_{12}^2$ and $M_2^2 = (k_3 + k_4)^2 \equiv k_{34}^2$ are of

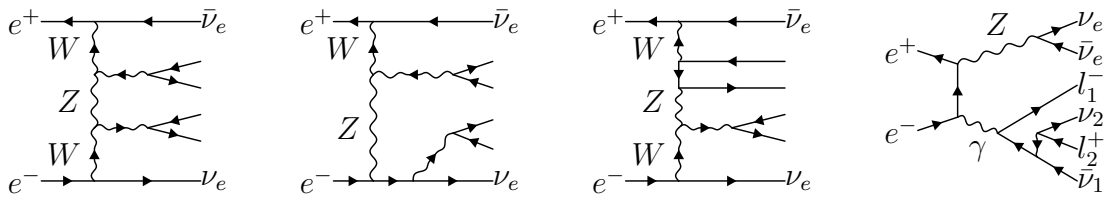

Figure 2: A few diagrams contributing to the process $e^+e^- \to \nu_e\, 4f\, \bar{\nu}_e$.

the order $\mathcal{O}(s^0) = \mathcal{O}(M_W^2)$. Inside the subprocess: $q_1 + q_2 \to k_{12} + k_{34}$ we consider the high energy limit $\hat{s} \gg t_1,\, t_2,\, M_1^2,\, M_2^2,\, \hat{t} = (q_1 - k_{12})^2 \equiv q^2$, where $\hat{t} = \mathcal{O}(s^0)$. Bounds on the Higgs mass which follow from unitarity constraints, usually, are studied in the fixed angle limit, $\hat{s} \sim \hat{t}$. In this paper we prefer the Regge limit, $\hat{s} \gg \hat{t}$. In this kinematic region the scattering amplitudes for vector - vector scattering take a particularly simple factorized form. Further below we will briefly indicate how the known results for on-shell scattering, derived in the fixed-angle limit, can be re-derived also in the Regge limit. As an important feature of the kinematic limit which we are going to investigate, the momentum transfer $\hat{t}$ of the subsystem is always negative and never reaches 0. The minimal value of $|\hat{t}|$, $-\hat{t}_{\min}$, is given by:

$$\hat{t}_{\min} = \frac{(t_1 - M_1^2)(t_2 - M_2^2)}{\hat{s}} + \mathcal{O}\left(\hat{s}^{-2}\right). \tag{1}$$

Here the leading term is always less or equal to zero, since

$$t_1, t_2 < m_e^2 \quad \text{and} \quad M_1^2, M_2^2 > m_e^2. \tag{2}$$

In the sum of all graphs which contribute to the matrix element we retain only those which, in the multi-Regge limit, contribute to the leading power of energy. This includes the diagrams with vector bosons in the exchange channel (Fig.2a,b,c) and eliminates those where fermions are exchanged (Fig.2d). Furthermore, we distinguish between 'resonant' (Fig.2a,b) and 'nonresonant' (Fig.2c) graphs: the former ones contain a W pole in the M_1 and in the M_2 channel, whereas the latter ones do not. Omitting the graphs of type 2b or 2c would lead to incorrect gauge dependent results.

The sum of all graphs which contribute to the multi-Regge limit can be written in the simple factorizing form:

$$\begin{aligned} T^{(s)}_{2\to 4\to 6} = &-2s\Gamma_{l\nu W}\frac{1}{t_1 - M_W^2} \\ &\left[\frac{\Gamma_{WZ(W\to\nu_1\, l_1^+)}(q_1, -q, k_1, k_2)}{M_1^2 - M_W^2}\,\frac{1}{\hat{t} - M_Z^2}\,\frac{\Gamma_{ZW(W\to l_2^-\bar{\nu}_2\,)}(q, q_2, k_3, k_4)}{M_2^2 - M_W^2}\right. \\ &\left. + \frac{\Gamma_{W\gamma(W\to\nu_1\, l_1^+)}(q_1, -q, k_1, k_2)}{M_1^2 - M_W^2}\,\frac{1}{\hat{t}}\,\frac{\Gamma_{\gamma W(W\to l_2^-\bar{\nu}_2\,)}(q, q_2, k_3, k_4)}{M_2^2 - M_W^2}\right]\frac{1}{t_2 - M_W^2}\Gamma_{l\nu W}. \end{aligned} \tag{3}$$

Here $\Gamma_{l\nu W}$ denotes the coupling of the virtual W boson to the incident electron or positron. In the high energy limit the helicity flip amplitudes are supressed. Therefore, the coupling contains a helicity conserving Kronecker $\delta_{\lambda\lambda'}$ where λ (λ') refer to the incoming (outgoing) fermion. Since W bosons only couple to left handed fermions, an additional $\delta_{\lambda,-}$ appears. Other vector scattering processes, such as $WW \to ZZ$, $\gamma\gamma \to WW$, or $WZ \to WZ$ factorize in the same way. We therefore present the results for these couplings in a general form which is applicable also to these processes. Because of its different couplings to left and right handed fermions, the emission of a virtual Z has a term proportional to $\delta_{\lambda,-}$, and another one proportional to $\delta_{\lambda,+}$ The emission of a virtual photon, on the other hand, is chiral invariant. We obtain:

$$\Gamma_{l\nu W} = \frac{g_w}{\sqrt{2}}\delta_{\lambda\lambda'}\delta_{\lambda,-} \qquad \Gamma_{llZ} = \frac{g_w}{2c_w}\delta_{\lambda\lambda'}\left((s_w^2 - c_w^2)\delta_{\lambda,-} + 2s_w^2\delta_{\lambda,+}\right) \qquad \Gamma_{ll\gamma} = g_w s_w \delta_{\lambda\lambda'}, \tag{4}$$

where $s_w = \sin\Theta_W$ and $c_w = \cos\Theta_W$ are our shorthand notations for the sine and cosine of the Weinberg angle, and g_w denotes the weak coupling constant which is connected to the Fermi constant G_F via $\frac{g_w^2}{8M_W^2} = \frac{G_F}{\sqrt{2}}$.

Next we turn to the effective production vertices on the rhs of (3). For the general subprocess $V_1V_2 \to V_3 \to f_a\bar{f}_b$ (Fig.3) it is of the form:

$$\Gamma_{V_1V_2(V_3\to f_a\bar{f}_b)}(p_1,p_2,p_a,p_b) = \chi\widehat{\Gamma}^{\rho}_{V_1V_2V_3}\bar{u}_{f_a}\gamma_\rho dv_{\bar{f}_b} + \left((p_1+p_2)^2 - M_{V_3}^2\right)\Gamma'_{V_1V_2(V_3\to f_a\bar{f}_b)}. \tag{5}$$

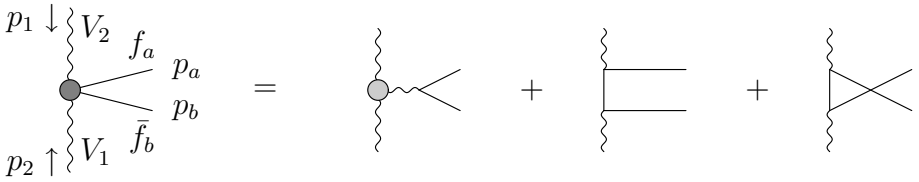

Figure 3: The effective vertex $\Gamma_{V_1V_2(V_3\to f_a\bar{f}_b)}(p_1,p_2,p_a,p_b)$

Here V_1 and V_2 are the upper and the lower 'incoming' virtual vector bosons with momenta p_1, p_2 and masses M_{V_1}, M_{V_2}, resp. The part $\widehat{\Gamma}^{\rho}_{V_1V_2V_3}$ on the rhs of eq.(5) contains the 'resonant' graphs with a particle pole of the produced vector boson, while $\Gamma'_{V_1V_2(V_3\to f_a\bar{f}_b)}$ stands for the 'nonresonant' ones (last two diagrams of figure 3). The analytic form of $\widehat{\Gamma}^{\rho}_{V_1V_2V_3}$ is [10]:

$$\widehat{\Gamma}^{\rho}_{V_1V_2V_3} = (p_{1\perp} - p_{2\perp})^\rho - \left(\alpha_1 + 2\frac{p_1^2 - M_{V_1}^2}{\beta_2 s}\right)p_A^\rho + \left(\beta_2 + 2\frac{p_2^2 - M_{V_2}^2}{\alpha_1 s}\right)p_B^\rho. \tag{6}$$

Here we have made use of the Sudakov decomposition of the momenta $p_i = \alpha_i p_A + \beta_i p_B + p_{i\perp}$. The coefficients χ denote the triple vector boson coupling constant:

$$\chi(WZ(W \to \nu_1\, l_1^+)) = g_w c_w \qquad \chi(W\gamma(W \to \nu_1\, l_1^+)) = -\, g_w s_w. \tag{7}$$

All other couplings χ can be obtained by using the relations $\chi(V_1V_2V_3) = \chi(V_2V_3V_1)$ and $\chi(V_1V_2V_3) = -\chi(V_2V_1V_3)$. The γ-matrices d describe the coupling of V_3 to its decay products:

$$\begin{aligned} d\left(W^+ \to \nu l^+\right) = d\left(W^- \to l^- \bar{\nu}\right) =& \frac{g_w}{\sqrt{2}}\omega_L \\ d\left(Z \to \nu\bar{\nu}\right) =& \frac{g_w}{2c_w}\omega_L \\ d\left(Z \to l^- l^+\right) =& \frac{g_w}{2c_w}\left((s_w^2 - c_w^2)\omega_L + 2s_w^2\omega_R\right) \\ d\left(\gamma \to l^- l^+\right) =& g_w s_w, \end{aligned} \tag{8}$$

where $\omega_L = \frac{1}{2}(1-\gamma_5)$ ($\omega_R = \frac{1}{2}(1+\gamma_5)$) project on the left handed (right handed) spinors.

For the nonresonant production vertex we find:

$$\Gamma'_{V_1V_2(V_3\to f_a\bar{f}_b)} = \bar{u}_{f_a}\left(\kappa_1 \frac{\underline{p_{\bar{f}_b}} - \underline{p_1}}{(p_{\bar{f}_b} - p_1)^2} + \kappa_2 \frac{\underline{p^\star_{f_a}} - \underline{p^\star_1}}{(p_{f_a} - p_1)^2}\right)\omega_L v_{\bar{f}_b}. \tag{9}$$

In this expression we have introduced the convention $\underline{p} = (p_x + ip_y)(\gamma^1 - i\gamma^2)$, $\underline{p}^\star = (p_x - ip_y)(\gamma^1 + i\gamma^2)$. The coefficients κ_1 and κ_2 are given by

$$\begin{aligned} \kappa_1\left(WZ\nu l^+\right) = \kappa_1\left(ZWl^-\bar{\nu}\right) =& \frac{g_w^2}{2\sqrt{2}c_w} \\ \kappa_2\left(WZ\nu l^+\right) = \kappa_2\left(ZWl^-\bar{\nu}\right) =& \frac{g_w^2 c_w(2M_W^2 - M_Z^2)}{2\sqrt{2}M_W^2} \\ \kappa_1\left(W\gamma\nu l^+\right) = \kappa_1\left(\gamma Wl^-\bar{\nu}\right) =& 0 \\ \kappa_2\left(W\gamma\nu l^+\right) = \kappa_2\left(\gamma Wl^-\bar{\nu}\right) =& -\frac{g_w^2 s_w}{\sqrt{2}} \\ \kappa_1\left(W^{(+)}W^{(-)}\nu\bar{\nu}\right) = \kappa_2\left(W^{(+)}W^{(-)}l^-l^+\right) =& 0 \\ \kappa_2\left(W^{(+)}W^{(-)}\nu\bar{\nu}\right) =& -g_w^2\frac{2M_W^2 - M_Z^2}{2M_W^2} \\ \kappa_1\left(W^{(+)}W^{(-)}(Z\to l^-l^+)\right) =& g_w^2 c_w^2 \frac{2M_W^2 - M_Z^2}{2M_W^2} \\ \kappa_1\left(W^{(+)}W^{(-)}(\gamma\to l^-l^+)\right) =& g_w^2 s_w^2, \end{aligned} \tag{10}$$

where the remaining couplings κ_1 and κ_2 can be constructed via $\kappa_1(V_1V_2f_a\bar{f}_b) = -\kappa_2(V_2V_1f_a\bar{f}_b)$.

With these building blocks it is easy to construct the scattering amplitudes for all off-shell vector boson scattering processes in the multi-Regge limit. Elastic WW scattering is a subprocesss of the process $e^+e^- \to \bar{\nu}_e(\nu l^+)(l^-\bar{\nu})\nu_e$, and the amplitude has already been given in (3). The subprocesses $WW \to ZZ$ and $WW \to \gamma\gamma$ are contained in the $2 \to 6$ process $e^+e^- \to \bar{\nu}_e(l_1^-l_1^+)(l_2^-l_2^+)\nu_e$. The corresponding $2 \to 6$ scattering amplitudes

are:

$$-2s\Gamma_{l\nu W}\frac{1}{t_1-M_W^2}\left[\frac{\Gamma_{WW(Z\to l_1^-l_1^+)}(q_1,-q,k_1,k_2)}{M_1^2-M_Z^2}\frac{1}{\hat{t}-M_W^2}\frac{\Gamma_{WW(Z\to l_2^-l_2^+)}(q,q_2,k_3,k_4)}{M_2^2-M_Z^2}\right]\frac{1}{t_2-M_W^2}\Gamma_{l\nu W}, \quad (11a)$$

$$-2s\Gamma_{l\nu W}\frac{1}{t_1-M_W^2}\left[\frac{\Gamma_{WW(\gamma\to l_1^-l_1^+)}(q_1,-q,k_1,k_2)}{M_1^2}\frac{1}{\hat{t}-M_W^2}\frac{\Gamma_{WW(\gamma\to l_2^-l_2^+)}(q,q_2,k_3,k_4)}{M_2^2}\right]\frac{1}{t_2-M_W^2}\Gamma_{l\nu W}. \quad (11b)$$

Similarly, the subprocesses $ZZ \to WW$ and $\gamma\gamma \to WW$ are part of the $2 \to 6$ process $e^+e^- \to e^+(\nu_1 l_1^+)(l_2^-\bar{\nu}_2)e^-$, and their scattering amplitudes are:

$$-2s\Gamma_{llZ}\frac{1}{t_1-M_Z^2}\left[\frac{\Gamma_{ZW(W\to\nu_1 l_1^+)}(q_1,-q,k_1,k_2)}{M_1^2-M_W^2}\frac{1}{\hat{t}-M_W^2}\frac{\Gamma_{WZ(W\to l_2^-\bar{\nu}_2)}(q,q_2,k_3,k_4)}{M_2^2-M_W^2}\right]\frac{1}{t_2-M_Z^2}\Gamma_{llZ}, \quad (12a)$$

$$-2s\Gamma_{ll\gamma}\frac{1}{t_1}\left[\frac{\Gamma_{\gamma W(W\to\nu_1 l_1^+)}(q_1,-q,k_1,k_2)}{M_1^2-M_W^2}\frac{1}{\hat{t}-M_W^2}\frac{\Gamma_{W\gamma(W\to l_2^-\bar{\nu}_2)}(q,q_2,k_3,k_4)}{M_2^2-M_W^2}\right]\frac{1}{t_2}\Gamma_{ll\gamma}. \quad (12b)$$

Finally, the subprocesses $WZ \to ZW$, $WZ \to \gamma W$, $W\gamma \to ZW$ and $W\gamma \to \gamma W$ are contained in the $2 \to 6$ scattering processes $e^+e^- \to \bar{\nu}_e(l_1^-l_1^+)(\nu_2 l_2^+)e^-$. The corresponding scattering amplitudes can be constructed from the vertices listed above. Note that vector boson scattering processes which are made up of just Z's and γ's, such as $\gamma\gamma \to ZZ$, do not exist on the tree level but require at least one loop.

As we have said before, inside these physical $2 \to 6$ inelastic processes the $2 \to 2$ vector-vector scattering processes appear as off-shell subprocesses, and they contain both longitudinal and transverse polarizations of the vector bosons. As an example, let us take the $2 \to 6$ process in eq.(3), and consider the effective production vertex in (6). As explicitly shown in [11], the produced W vector boson, in the overall center of mass system, can have both transverse or longitudinal polarization. Transforming to the center of mass system of the produced pair of W bosons, we still have all three polarization states of the two W bosons. Moving on to the particle poles in the t_1 and t_2 channels and making use of helicity conservation, we conclude that we are dealing with a superposition of transverse and longitudinally polarized vector bosons, both in the 'incoming' t_1 and t_2 channels and in the 'outgoing' M_1 and M_2 channels.

A separation of the different polarization starts from the angular distribution of the two fermion decay of the 'outgoing' vector boson. Let us again consider the $WW \to WW$

process contained in eq.(3). Moving into the rest frame of one of the 'outgoing' W bosons, and denoting the decay angles of the two decay products by θ_i and $\pi - \theta_i$, the decay amplitude of an on-shell transversal polarized W behaves like $1 \pm \cos\theta_i$, while for a logitudinal polarized W it is proportional to $\sin\theta_i$ [12, 13]. Hence, by a suitable projection we can separate the different outgoing polarization states. An analogous statement holds also for 'outgoing' Z bosons. By further making use of helicity conservation at the effective production vertex, this separation of polarization extends also to the 'incoming' vector bosons of the quasielastic subprocess. This brief argument illustrates that, by analysing the angular distribution of the decay products of the 'outgoing' vector boson and by moving onto the particle poles in the t_i and M_i channels, it is possible to regain the usual on-shell vector-vector scattering amplitudes and, in particular, to isolate longitudinal vector-vector scattering.

Let us finally return to the specific case of WW scattering. In section 3, as a first application of our formulae, we will be interested in the dependence on the Higgs mass at high energies. In the absence of the Higgs contribution, (3) is replaced by

$$\begin{aligned} T_{2\to4\to6}^{(s,\text{withoutHiggs})} = & -2s\Gamma_{l\nu W}\frac{1}{t_1 - M_W^2} \\ & \left[\frac{\Gamma_{WZ(W\to\nu_1\, l_1^+)}(q_1,-q,k_1,k_2)}{M_1^2 - M_W^2}\,\frac{1}{\hat{t} - M_Z^2}\,\frac{\Gamma_{ZW(W\to l_2^-\bar{\nu}_2\,)}(q,q_2,k_3,k_4)}{M_2^2 - M_W^2}\right. \\ & + \frac{\Gamma_{W\gamma(W\to\nu_1\, l_1^+)}(q_1,-q,k_1,k_2)}{M_1^2 - M_W^2}\,\frac{1}{\hat{t}}\,\frac{\Gamma_{\gamma W(W\to l_2^-\bar{\nu}_2\,)}(q,q_2,k_3,k_4)}{M_2^2 - M_W^2} \\ & \left. - g_w^2 M_W^2 \frac{\bar{u}_{\nu_1}\gamma_\mu dv_{l_1^+}}{M_1^2 - M_W^2}\,\frac{\bar{u}_{l_2^-}\gamma^\mu dv_{\bar{\nu}_2}}{M_2^2 - M_W^2}\right]\frac{1}{t_2 - M_W^2}\Gamma_{l\nu W}. \end{aligned} \tag{13}$$

Comparing (3) with (13) one easily sees that the presence of the Higgs particle affects the dependence upon $\hat{t}$: in the large $\hat{t}$ region the renormalizibility of the electroweak theory requires the amplitude to vanish, and it is the Higgs particle which cancels the constant term in square bracket term in (13). We illustrate this effect of the Higgs mass numerically in Fig.4: the ratio of $\frac{d\sigma}{dt}$ for the theory without Higgs vs. the theory with Higgs becomes large when $\hat{t}$ exceeds M_W^2. For this plot we choose $M_H = 115\text{GeV}$, and the phase space integration covers the region $t_1, t_2 \in [-M_W^2, -.01M_W^2]$, $\delta_1 = \frac{M_1^2 - M_W^2}{M_W^2}$, $\delta_2 = \frac{M_2^2 - M_W^2}{M_W^2} \in [.025, .1]$, $\sqrt{\hat{s}} \in [400\text{GeV}, 500\text{GeV}]$, $s_{01234} \in [400\text{GeV}, 750\text{GeV}]$ where $s_{01234} = (p'_A + k_{12} + k_{34})^2$.

For a heavy Higgs it is instructive to consider also next-to-leading contributions to (3) which are suppressed by a factor $\frac{M_H^2}{\hat{s}}$. It is these terms which will lead to a conflict with the unitarity bounds once the Higgs become too heavy. For the case of $WW \to WW$ scattering we find:

$$T_{2\to4\to6}^{(H)} = -2s\Gamma_{l\nu W}\frac{1}{t_1 - M_W^2}\left[\frac{g_w^2 M_W^2 M_H^2}{\hat{s}}\,\frac{\bar{u}_{\nu_1}\gamma_\mu dv_{l_1^+}}{M_1^2 - M_W^2}\,\frac{\bar{u}_{l_2^-}\gamma^\mu dv_{\bar{\nu}_2}}{M_2^2 - M_W^2}\right]\frac{1}{t_2 - M_W^2}\Gamma_{l\nu W}. \tag{14}$$

The analogous Higgs mass dependent next-to-leading expressions for two other processes,

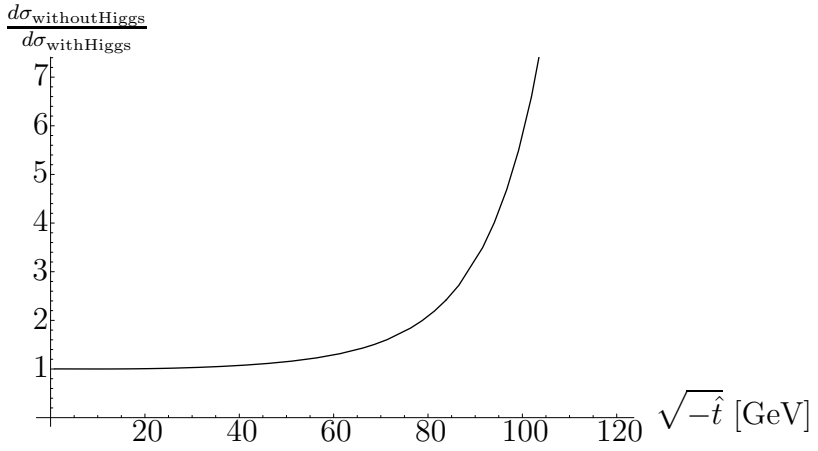

Figure 4: The $\hat{t}$ dependence of the ratio of $\frac{d\sigma}{d\hat{t}}$.

namely for $WW \to ZZ$ scattering inside the $2 \to 6$ process (11a):

$$-2s\Gamma_{l\nu W}\frac{1}{t_1 - M_W^2}\left[\frac{g_w^2 M_W^2 M_H^2}{\hat{s}}\ \frac{\bar{u}_{l_1^-} d_\mu v_{l_1^+}}{M_1^2 - M_Z^2}\ \frac{\bar{u}_{l_2^-} d^\mu v_{l_2^+}}{M_2^2 - M_Z^2}\right]\frac{1}{t_2 - M_W^2}\Gamma_{l\nu W} \tag{15}$$

and for $ZZ \to WW$ scattering inside (12a) are:

$$-2s\Gamma_{llZ}\frac{1}{t_1 - M_Z^2}\left[\frac{g_w^2 M_W^2 M_H^2}{\hat{s}}\ \frac{\bar{u}_{\nu_1} d_\mu v_{l_1^+}}{M_1^2 - M_W^2}\ \frac{\bar{u}_{l_2^-} d^\mu v_{\bar{\nu}_2}}{M_2^2 - M_W^2}\right]\frac{1}{t_2 - M_Z^2}\Gamma_{llZ}. \tag{16}$$

3 Unitarity Bounds

As a first application of our analytic expressions, we reconsider the derivation of unitarity bounds on the Higgs mass; in contrast to earlier discussions in the literature which did not include the photon pole we will examine the influence of the photon pole. As we will discuss in detail, our discussion will be much less rigorous than the traditional arguments based upon on-shell scattering.

We start by showing, for on-shell vector-vector scattering, how the usual investigation of the fixed-angle limit can be carried out also in the Regge limit. Unitarity of the $2 \to 2$ scattering process is illustrated in Fig. 5. The signs within the bubbles indicate on which side of the branch cut in the complex s plane the amplitudes has to be evaluated. A "+" marks the value above the cut, $s\underline{+i\epsilon}$, a "−" below the cut, $s\underline{-i\epsilon}$. Projecting on the partial waves one arrives at the inequality:

Figure 5: unitarity of $2 \to 2$ scattering

$$\Im\mathrm{m} T_l^{(el)} = \left|T_l^{(el)}\right|^2 + \sum_n \left|T_l^{(inel)}\right|^2 \tag{17}$$

$$\Rightarrow \quad \left|T_l^{(el)}\right| \geq \left|\Im\mathrm{m} T_l^{(el)}\right| \geq \left|T_l^{(el)}\right|^2 \tag{18}$$

$$\Rightarrow \quad \left|T_l^{(el)}\right| \leq 1. \tag{19}$$

Lee, Quigg and Thacker [1] have used this inequality in order to derive, from the elastic scattering of longitudinal polarized W bosons, an upper bound on the Higgs mass. The $l = 0$ partial wave is obtained from the fixed-angle limit of the elastic scattering amplitude, and in the absence of a Higgs particle it has the form:

$$T_0^{(\text{withoutHiggs})}(W_L^+ W_L^-) = \frac{g_w^2}{128\pi} \frac{s}{M_W^2} + \mathcal{O}\left(s^0\right). \tag{20}$$

For energies of the order $\sqrt{s} \simeq 16\sqrt{\frac{\pi}{2}}\frac{M_W}{g_w} \approx 2.4\text{TeV}$ the inequality (19) is violated, and the W's start to interact strongly [14]. Once the Higgs is included, the term proportional to s cancels. But even though the $l = 0$ partial wave is no longer growing with s, this does not automatically imply that it is smaller than 1. Lee, Quigg and Thacker calculated the matrix element in the fixed angle limit using the equivalence theorem [2, 4] and found that the 0th partial wave is proportional to the Higgs mass squared:

$$T_0^{(\text{withHiggs})}(W_L^+ W_L^-) = \frac{g_w^2}{32\pi} \frac{M_H^2}{M_W^2} + \mathcal{O}\left(s^{-1}\right). \tag{21}$$

The inequality (19) leads to the condition $M_H < 8\sqrt{\frac{\pi}{2}}\frac{M_W}{g_w} \approx 1.2\text{TeV}$. This bound can be made more stringent if the scattering channels ZZ and HH are included. One finds $\Rightarrow M_H < 8\sqrt{\frac{\pi}{3}}\frac{M_W}{g_w} \approx 1.0\text{TeV}$. In this discussion the photon exchange had not been included. As function of the scattering angle, the photon propagator goes like $\sim \frac{1}{1-\cos\theta}$, and the partial wave projection is not defined, unless the region $\theta \sim 0$ is excluded.

It is not difficult to derive the bound on the Higgs particle also from the Regge limit: $s \to \infty$, t fixed (i.e. $\theta \to 0$). Instead of the partial wave we define the Fourier transform with respect to impact parameter $\boldsymbol{b}$:

$$\widetilde{T}(s,b) = \frac{1}{16\pi^2 s} \int d^2\boldsymbol{q} e^{-i\vec{q}_\perp \vec{b}} T(s,t). \tag{22}$$

Within this representation the unitarity relation can be simplified in a way similar to the partial wave decomposition:

$$\Im\mathrm{m}\widetilde{T}(s,b)^{(el)} = \left|\widetilde{T}(s,b)^{(el)}\right|^2 + \sum_n \left|\widetilde{T}(s,b)^{(inel)}\right|^2 \tag{23}$$

$$\Rightarrow \quad \left|\widetilde{T}(s,b)^{(el)}\right| \leq 1. \tag{24}$$

In the Regge limit the matrix element for $W_L^+W_L^-$ scattering without a Higgs contribution reads:

$$\begin{aligned} T^{(\text{withoutHiggs})} = & -2g_w^2 s\left[\frac{c_w^2}{t-M_Z^2}\left(\frac{2M_W^2-M_Z^2}{2M_W^2}\right)^2 + \frac{s_w^2}{t}\right] \\ & -\frac{g_w^2 s}{2M_W^4}\left[-\frac{M_W^2}{2}\right] + \mathcal{O}\left(s^0\right). \end{aligned} \tag{25}$$

Ignoring, for the time being, the photon pole, one sees that the violation of unitarity now arises due to the the large-t behavior: since in the b-transform the $\boldsymbol{q}$-integral can not be extended to infinity, we have to remember that $-t_{\max} = s - 4M_W^2$. The b transform now grows with s and violates the unitarity bound. Once the Higgs is included the scattering amplitude takes the form

$$\begin{aligned} T^{(\text{withHiggs})} = & -2g_w^2 s\left[\frac{c_w^2}{t-M_Z^2}\left(\frac{2M_W^2-M_Z^2}{2M_W^2}\right)^2 + \frac{s_w^2}{t}\right] \\ & -\frac{g_w^2}{2M_W^4}\left[\frac{M_H^2 M_W^2}{2}\right] + \mathcal{O}\left(s^0 M_H^0\right). \end{aligned} \tag{26}$$

The term proportional to s now vanishes as $\hat{t}$ becomes large. As a consequence, the $\boldsymbol{q}$-integral converges, with the exception of the point $\boldsymbol{b} = 0$: at this point the b-transform grows as $\ln s/M_W^2$, but this contribution becomes significant only at energies much higher than the TeV-region and, in our discussion, can safely be neglected. For a heavy Higgs, however, the second term in (26) becomes significant: the contribution from $-t \sim s - 4M_W^2$ exceeds unity unless the Higgs mass stays below the upper limit which is the exactly the same (cf. eq.(21)) one as the one obtained by Lee, Quigg, and Thacker. As in the fixed angle limit, the photon pole can not be included, since the b integral diverges at $\boldsymbol{q} = 0$.

Turning now to the off-shell scattering of vector bosons, we immediateley see that it is the $\hat{t}_{\min}$ in eq.(1) which excludes the dangerous photon pole. The question we are interested in is the influence of the photon exchange on the unitarity bound of the Higgs mass. In order to derive a unitarity bound we have to consider the singularity structure of six-point amplitude $T_{2\to 6}$ in the energy variable $\hat{s}$ which plays the role of the energy of the WW scattering subprocess. The corresponding unitarity integral is illustrated in Fig.6.

Again, the '$\pm$' signs denote on which side of the branch cut the amplitudes have to be evaluated. The intermediate states on the rhs of the unitarity equation consist of stable particles. Since, in our off-shell discussion, the W boson has to be treated as unstable

Figure 6: unitarity of $2 \to 6$ scattering

[15], the sum over intermediate states has to extend over the stable decay products of the W boson, which, to lowest order, consists of a pair of leptons, $(l\nu)$. In our figure, we have marked the cut through the self energy by the a blob with a vertical cutting line. The W propagators on the rhs and on the lhs of this cut blob contain the self energies, i.e. the poles are slightly off the real axis. While in the unitarity integral the decay products of the W boson are kept on-shell, their momenta are integrated over. As a result, the sqares of the four momentum of the W bosons, $k_{12}^2 = M_1^2$ and $k_{34}^2 = M_2^2$, also vary. Moreover, they are real-valued and thus never reach the W pole in the complex plane.

All this discussion applies to a situation where all orders in perturbation theory are taken into account. Our discussion is carried out in lowest order perturbation theory: in this approximation the W pole lies on the real axis, and intermediate state on the rhs in Fig. 6 reduces to the W boson. Nevertheless, thanks to the off-shellness of the 'incoming' and 'outgoing' W bosons, $\hat{t}_{\min}$ stays below zero, and the integration over the intermediate state momenta leads to logarithm of $\hat{t}_{\min}$. In order to be as close as possible to the realistic situation, we will chose $k_{12}^2 = M_1^2$ and $k_{34}^2 = M_2^2$ to differ from M_W^2 by a characteristic size $\Gamma_W M_W$.

In contrast to the $2 \to 2$ on-shell scattering it is not possible to derive, on general grounds, a rigorous inequality analogous to (19) or (24). Since the scattering amplitude $T_{2\to 6}$ depends upon several energy variables with nonvanishing discontinuities, the discontinuity in $\hat{s}$ does not coincide with the imaginary part. All we can say is that, in leading order in s/M_W^2 and in M_H^2/M_W^2, the scattering amplitude of our process, $T_{2\to 6}$, is real-valued; all energy discontunities are suppressed by one power in g_W^2. The imaginary part is a sum of energy discontinuities. Because of the linear independence of the different energy discontinuities, a large discontinuity in $\hat{s}$ can not be compensated by a discontinuity in another energy variable: a too strong growth of the discontinuity in $\hat{s}$, therefore, should certainly be viewed as indicative of violation of unitarity.

Furthermore, the 'inelastic' contribution on the rhs of the discontinuity equation (Fig.6) for $T_{2\to 6}$ can no longer be written as a sum of squares. Its contribution to the unitary sum could, in principle, have the opposite sign compared to the elastic intermediate state; this, however, would require a rather dramatic difference between the on-shell WW scattering amplitude and the off-shell situation. When starting from the W-poles in the t_1, t_2, M_1^2, and M_2^2 channels, our $T_{2\to 6}$ amplitude contains the on-shell WW scattering amplitude which, in its own energy discontinuity, contains a positive inelastic contribution. Moving away from these poles, the inelastic contribution to the discontinuity in $\hat{s}$ would have to decrease, pass through zero and become negative. This would be fairly strong variation.

Finally a remark on the polarization. As we have discussed before, the $2 \to 6$ amlitudes

on the lhs of Fig.6 contains both longitudinal and transverse polarizations of the produced vector bosons. By a suitable analysis of the angular distribution of the fermion pair one could isolate the longitudinal part; in our subsequent estimate of the effect of the photon pole we will not do this. On the other hand, in the intermediate states on the rhs of the unitarity equation in Fig.6 , we will restrict ourselves to longitudinal polarized W bosons only. We expect that, as far as the unitarity bound for large Higgs masses is concerned, the neglect of the transverse polarized intermediate states which are not affected by the Higgs mass will be a small effect.

Summing up this discussion, it seems plausible (but not proven) that we still can use the inequality

$$\left|\widetilde{T}_{2\to 4\to 6}(\hat{b})\right| \geq \left|\widetilde{T}_{2\to 4}(\hat{b})\widetilde{T}_{2\to 2\to 4}(\hat{b})\right|, \tag{27}$$

where $T_{2\to 4}$ denotes the process $e^+e^- \to \bar{\nu}_e W_L^+ W_L^- \nu_e$, and $T_{2\to 2\to 4}$ stands for the process $W_L^+W_L^- \to \nu_1 l_1^+ l_2^- \bar{\nu}_2$. The 'impact parameter' vector $\hat{\boldsymbol{b}}$ belongs to the exchange in the WW-subsystem. In the following we shall examine and numerically estimate the role of the photon pole in (27).

The kinematic variables of the $2 \to 4$-process $e^+(p_A)e^-(p_B) \to \bar{\nu}_e(p'_A)W_L^+(\tilde{q}_1)W_L^-(\tilde{q}_2)\nu_e(p'_B)$ are the same as those of the $2 \to 6$-process, except for the outgoing states of the subsystem which are shown in figure 7. The momentum transfer $\hat{t}'$ in the WW subsystem is given by $\hat{t}' \equiv {q'}^2 \equiv (q_1 - \tilde{q}_1)^2$. The momentum transfer $\hat{t}''$ in the $2 \to 4$-process $W_L^+(\tilde{q}_1)W_L^-(\tilde{q}_2) \to \nu_1(k_1)l_1^+(k_2)l_2^-(k_3)\bar{\nu}_2(k_4)$ is given by $\hat{t}'' \equiv \tilde{q}^2 \equiv (\tilde{q}_1 - (k_1 + k_2))^2$. The scattering amplitudes which enter the lhs of (27) can be extracted from the corresponding $2 \to 6$ process (3) which are described in section 2.

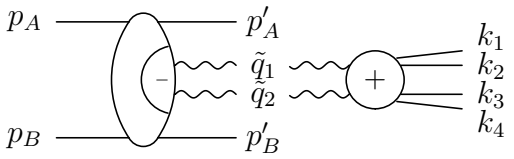

Figure 7: kinematics of $T_{2\to 4}$ and $T_{2\to 2\to 4}$

Let us make a few remarks on the kinematics. First we notice that, on both sides of eq.(27), we have the denominators $(t_1 - M_W^2)$, $(t_2 - M_W^2)$, and $(M_1^2 - M_W^2)$, $(M_1^2 - M_W^2)$. It is convenient to define new functions $\widetilde{\mathcal{T}}(\hat{b})$:

$$\widetilde{\mathcal{T}}_{2\to 4\to 6} = \frac{\hat{s}}{s}(t_1 - M_W^2)(t_2 - M_W^2)(M_1^2 - M_W^2)(M_2^2 - M_W^2)\widetilde{T}_{2\to 4\to 6} \tag{28}$$

$$\widetilde{\mathcal{T}}_{2\to 4} = \frac{\hat{s}}{s}(t_1 - M_W^2)(t_2 - M_W^2)\widetilde{T}_{2\to 4} \tag{29}$$

$$\widetilde{\mathcal{T}}_{2\to 2\to 4} = (M_1^2 - M_W^2)(M_2^2 - M_W^2)\widetilde{T}_{2\to 2\to 4}, \tag{30}$$

where, for brevity, we have dropped the dependence upon b. Inserting these functions into (27) we obtain:

$$|\widetilde{\mathcal{T}}_{2\to 4\to 6}| \geq |\widetilde{\mathcal{T}}_{2\to 4}\widetilde{\mathcal{T}}_{2\to 2\to 4}|. \tag{31}$$

Following the discussion of the on-shell elastic scattering amplitude, we begin with the case where the Higgs particle is absent, and we ignore the photon exchange. We consider the point $\boldsymbol{b} = 0$ which is most sensitive to the large-t behavior. On the lhs of (31) we find, from the constant terms in (13), that the large-$\hat{t}$ region leads to a growth proportional to $\hat{s}/M_W^2$. Similarly, on the rhs both the first and the second factor grow as $\hat{s}/M_W^2$ and violates the inequality which follows from unitarity. Once the Higgs particle is included the growth proportional to $\hat{s}/M_W^2$ disappears on both sides of (31). The Fourier transform to b space has to be done numerically; however it is not difficult to understand the general pattern by concentrating on those terms which become large as both M_H and $\hat{s}$ grow. To begin with the lhs, the term proportional to M_H^2 leads to a contribution which is constant in $\hat{s}$; its coefficient follows directly from (14). Next, the Z exchange in (3) leads to a term which grows proportional to $\ln M_Z^2/\hat{s}$. Finally, the photon exchange yields an additional term proportional to $\ln \hat{t}_{\min}/\hat{s}$ as well as terms proportional to $\ln \hat{t}_{\min}/M_W^2$ where $\hat{t}_{\min}$ is given in (1). The coefficient of the terms proportional to $\ln \hat{t}_{\min}/M_W^2$ has a somewhat complicated form and has to be evaluated numerically. On the rhs we find, for each of the two scattering ampltitudes, four terms of the same kind. As a result, our inequality (31) takes the form:

$$\frac{g_w^6}{32\pi}\left(M_H^2M_W^2 + c_w^2(2M_W^2 - M_Z^2)^2\ln\frac{M_Z^2}{\hat{s}} + 4s_w^2M_W^4\ln\frac{\hat{t}_{\min}}{\hat{s}} + C_1\ln\frac{\hat{t}_{\min}}{M_W^2}\right) \geq$$
$$\frac{g_w^4}{16\pi}\left(M_H^2 + c_w^2\frac{(2M_W^2 - M_Z^2)^2}{M_W^2}\ln\frac{M_Z^2}{\hat{s}} + 4s_w^2M_W^2\ln\frac{\hat{t}'_{\min}}{\hat{s}} + C_2\ln\frac{\hat{t}_{\min}}{M_W^2}\right)$$
$$\cdot\,\frac{g_w^4}{64\pi}\left(M_H^2 + c_w^2\frac{(2M_W^2 - M_Z^2)^2}{M_W^2}\ln\frac{M_Z^2}{\hat{s}} + 4s_w^2M_W^2\ln\frac{\hat{t}''_{\min}}{\hat{s}} + C_3\ln\frac{\hat{t}_{\min}}{M_W^2}\right), \quad (32)$$

where

$$\hat{t}'_{min} = \frac{(t_1 - M_W^2)(t_2 - M_W^2)}{\hat{s}},\ \hat{t}''_{min} = \frac{(M_1^2 - M_W^2)(M_2^2 - M_W^2)}{\hat{s}}. \quad (33)$$

The three positive coefficients C_i have to be computed numerically: In each of the three factors, the main contribution comes from the first term proportional to M_H^2: if the other terms would be ignored, the Higgs bound would be the same as in the on-shell case. The terms $\sim \ln \hat{t}_{\min}$, are due to the photon exchange; for small $\hat{t}_{\min}$, they have the opposite sign and they tend to weaken the bound on the Higgs mass.

Further results are obtained from a numerical analysis. By setting $\theta_i = \frac{\pi}{2}$ (see discussion on page 6) we make the longitudinal component of the outgoing off-shell W's maximal, i.e. we strengthen the sensitivity to the Higgs mass. Compared to the critical value of the Higgs mass, which is obtained in the on-shell analysis, 1234GeV, the bound in our off-shell analysis slightly increases up to the range between 1247GeV and 1252GeV (depending upon the values for $|t_1|$, $|t_2|$, and $|\delta_1|$, $|\delta_2|$ which are varied over the intervals described at the end of section 2). In the inequality (32), the contribution which is most sensitive to the photon exchange comes from the last term on the rhs $\propto \ln \frac{\hat{t}''_{\min}}{\hat{s}}$ with $\hat{t}''_{\min} = \frac{\delta_1\delta_2 M_W^4}{\hat{s}}$. For the considered ranges of δ_1, δ_2 and $\hat{s}$ the parameter $\hat{t}''_{\min}$ varies between .1Gev^2 and 2.6GeV^2. The rather weak dependence of the critical Higgs mass on δ_1 and δ_2 is illustrated in Fig. 8.

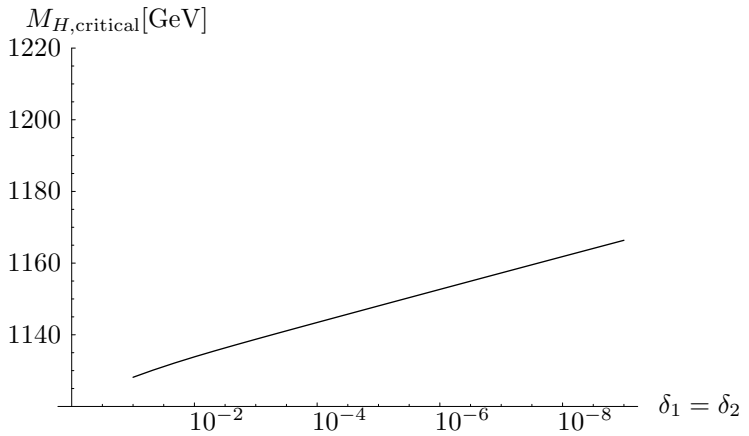

Figure 8: The critical Higgs mass as a function of $\delta_1 = \delta_2$ at $t_1 = t_2 = -M_W^2$, $\sqrt{\hat{s}} = 10^3$GeV.

We end this section by including into our numerical analysis the intermediate states of other weak vector bosons and of the Higgs boson. In the on-shell analysis, the bound on the Higgs mass becomes stronger once these vector and Higgs states have been included, not only in the intermediate states but also in the initial and final states. In our off-shell analysis we will not go quite as far, since different outgoing vector bosons also would affect the decays into fermion pairs. Instead, we stick to incoming and outgoing W's, and we only include additional Z's and Higgs particles in the intermediate states:

$$\left|\widetilde{\mathcal{T}}_{2\to4\to6}\right| \geq \left|\widetilde{\mathcal{T}}^{(WW)}_{2\to4}\widetilde{\mathcal{T}}^{(WW)}_{2\to2\to4} + \frac{1}{2}\widetilde{\mathcal{T}}^{(ZZ)}_{2\to4}\widetilde{\mathcal{T}}^{(ZZ)}_{2\to2\to4} + \frac{1}{2}\widetilde{\mathcal{T}}^{(HH)}_{2\to4}\widetilde{\mathcal{T}}^{(HH)}_{2\to2\to4}\right|. \tag{34}$$

Here the upper indices refer to the particles in the (longitudinal) intemediate states, e.g. $\widetilde{\mathcal{T}}^{(ZZ)}_{2\to4}$ belonges to the process $e^+e^- \to \bar{\nu}_e Z_L Z_L \nu_e$, whereas $\widetilde{\mathcal{T}}^{(ZZ)}_{2\to2\to4}$ is part of the process $Z_L Z_L \to \nu_1 l_1^+ l_2^- \bar{\nu}_2$. The kinematic variables for the process $e^+(p_A)e^-(p_B) \to \bar{\nu}_e(p'_A)Z_L(\tilde{q}_1)Z_L(\tilde{q}_2)\nu_e(p'_B)$ are the same as those of the $2 \to 6$-process, except for the outgoing states of the subsystem (momentum transfer $\hat{t}' \equiv q'^2 \equiv (q_1 - \tilde{q}_1)^2$). The matrix elements can be extracted from the associated $2 \to 6$-amplitude (11a) in the same way as in the $WW \to WW$ case. In the same we derive from (12a) the matrix element for the process $Z_L(\tilde{q}_1)Z_L(\tilde{q}_2) \to \nu_1(k_1)l_1^+(k_2)l_2^-(k_3)\bar{\nu}_2(k_4)$.

The matrix element for the process $e^+(p_A)e^-(p_B) \to \bar{\nu}_e(p'_A)H(\tilde{q}_1)H(\tilde{q}_2)\nu_e(p'_B)$ reads (momentum transfer $\hat{t}' \equiv q'^2 \equiv (q_1 - \tilde{q}_1)^2$):

$$T^{(HH)}_{2\to4} = 2s\Gamma_{l\nu W}\frac{1}{t_1 - M_W^2}\left[g_w M_W \frac{1}{(\hat{t}' - M_W^2)} g_w M_W + \frac{g_w^2 M_H^2}{2\hat{s}}\right]\frac{1}{t_2 - M_W^2}\Gamma_{l\nu W}. \tag{35}$$

The matrix element for the process $H(\tilde{q}_1)H(\tilde{q}_2) \to \nu_1(k_1)l_1^+(k_2)l_2^-(k_3)\bar{\nu}_2(k_4)$ reads (mo-

mentum transfer $\hat{t}'' \equiv \tilde{q}^2 \equiv (\tilde{q}_1 - (k_1 + k_2))^2$):

$$T^{(HH)}_{2\to 2\to 4} = 2\hat{s}\left[\frac{g_w M_W \bar{u}_{\nu_1}\gamma_\mu dv_{l_1^+}}{M_1^2 - M_W^2}\,\frac{1}{\hat{t}'' - M_W^2}\,\frac{g_w M_W \bar{u}_{l_2^-} d^\mu v_{\bar{\nu}_2}}{M_2^2 - M_W^2} + \frac{g_w^2 M_H^2}{2\hat{s}}\,\frac{\bar{u}_{\nu_1}\gamma_\mu dv_{l_1^+}}{M_1^2 - M_W^2}\,\frac{\bar{u}_{l_2^-} d^\mu v_{\bar{\nu}_2}}{M_2^2 - M_W^2}\right]. \tag{36}$$

In contrast to the coupling of Z exchange to incoming W bosons, $\Gamma_{WZ(W\to\nu_1 l_1^+)}$ in (5), the analogous vertex for incoming Higgs bosons are very simple because in all non resonant diagrams the Higgs couple to fermions. These couplings are proportional to the fermion masses, and they can be neglected in comparison with the gauge boson masses.

With the same kinematical parameters used before, in this extended analysis the critical Higgs mass lies between 1119GeV and 1126GeV, compared to the critical Higgs mass 1104GeV in the analogous on-shell analysis. The dependence upon $\hat{s}$ and δ_1, δ_1 is very much the same as in the previous single-channel analysis.

4 Conclusions

We have calulated analytic expressions for the matrix elements of off-shell scattering of weak vector bosons in the limit of large center of mass energies. Our off-shell scattering amplitudes are derived from the process $e^+e^- \to \bar{\nu}_e\nu_1 l_1^+ l_2^- \bar{\nu}_2\nu_e$ in the multi-Regge limit. The expressions have a simple factorized form and can be used for further theoretical studies of W^+W^- scattering. We also have calculated the related matrix elements for vector boson scattering processes composed of the channels WW, ZZ, $\gamma\gamma$, WZ, $W\gamma$, $Z\gamma$.

As an application, we have re-examinded the derivation of bounds on the Higgs mass from unitarity. In contrast to on-shell scattering, our off-shell analysis allows to include the photon exchange. We have given plausibility arguments which have lead us to an inequality, derived from unitarity. Based upon this inequality we have examined the influence of the photon exchange on the upper bound of the Higgs mass. As a result we have shown that the photon pole tends to weaken the bound on the Higgs mass. We have demonstrated numerically that the shift of the mass bound due to the photon is small compared to the general uncertainty of the bound derived from lowest order unitarity contribution.

References

[1] B. W. Lee, C. Quigg and H. B. Thacker, *Phys. Rev.*, **D 16** (1977) 1519.

[2] J. M. Cornwall, D. N. Levin and G. Tiktopoulos, *Phys. Rev.*, **D 10** (1974) 1145.

[3] S. Dawson, *Nucl. Phys.*, **B 249** (1985) 42.

[4] H. G. J. Veltman, *Phys. Rev.*, **D 41** (1990) 2294.

[5] V. D. Barger, K. Cheung, T. Han and R. J. N. Phillips, *Phys. Rev.*, **D 52** (1995) 3815 [arXiv:hep-ph/9501379].

[6] I. Kuss and H. Spiesberger, *Phys. Rev.*, **D 53** (1996) 6078 [arXiv:hep-ph/9507204].

[7] A. Denner and T. Hahn, *Nucl. Phys.*, **B 525** (1998) 27 [arXiv:hep-ph/9711302].

[8] F. Gangemi, G. Montagna, M. Moretti, O. Nicrosini and F. Piccinini, *Eur. Phys. J.*, **C 9** (1999) 31 [arXiv:hep-ph/9811437].

[9] S. Dittmaier and M. Roth, *Nucl. Phys.*, **B 642** (2002) 307 [arXiv:hep-ph/0206070].

[10] For equal masses see L. N. Lipatov, *Sov. J. Nucl. Phys.* **23** (1976) 338 [*Yad. Fiz* **23** (1976) 642].

[11] J. Bartels, *Nucl. Phys.*, **B 151** (1979) 293.

[12] K. Hagiwara, R. D. Peccei, D. Zeppenfeld and K. Hikasa, *Nucl. Phys.*, **B 282** (1987) 253.

[13] M. J. Duncan, G. L. Kane and W. W. Repko, *Nucl. Phys.*, **B 272** (1986) 517.

[14] M. S. Chanowitz, (1998) [arXiv:hep-ph/9812215].

[15] M. J. G. Veltman, *Physica*, **29** (1963) 186.

[16] R. J. Eden, P. V. Landshoff, D. I. Olive and J. C. Polkinghorne, *The analytic S-matrix*, Cambridge Univ. Pr, 1966.